



# Fermi National Accelerator Laboratory

FERMILAB-Conf-99/134-E

CDF and D0

## Diffractive Results from the Tevatron

Gilvan A. Alves

For the CDF and D0 Collaborations

*Lafex/CBPF*

*Rua Xavier Sigaud 150, 22290-180, Rio de Janeiro, RJ, Brasil*

*Fermi National Accelerator Laboratory*

*P.O. Box 500, Batavia, Illinois 60510*

May 1999

Published Proceedings of *DPF '99 American Physical Society Division of Particles and Fields*,  
University of California, Los Angeles, January 5-9, 1999

## **Disclaimer**

*This report was prepared as an account of work sponsored by an agency of the United States Government. Neither the United States Government nor any agency thereof, nor any of their employees, makes any warranty, expressed or implied, or assumes any legal liability or responsibility for the accuracy, completeness, or usefulness of any information, apparatus, product, or process disclosed, or represents that its use would not infringe privately owned rights. Reference herein to any specific commercial product, process, or service by trade name, trademark, manufacturer, or otherwise, does not necessarily constitute or imply its endorsement, recommendation, or favoring by the United States Government or any agency thereof. The views and opinions of authors expressed herein do not necessarily state or reflect those of the United States Government or any agency thereof.*

## **Distribution**

*Approved for public release; further dissemination unlimited.*

## **Copyright Notification**

*This manuscript has been authored by Universities Research Association, Inc. under contract No. DE-AC02-76CHO3000 with the U.S. Department of Energy. The United States Government and the publisher, by accepting the article for publication, acknowledges that the United States Government retains a nonexclusive, paid-up, irrevocable, worldwide license to publish or reproduce the published form of this manuscript, or allow others to do so, for United States Government Purposes.*

# Diffractive Results from the Tevatron

Gilvan A. Alves

*Lafex/CBPF*

*Rua Xavier Sigaud 150, 22290-180, Rio de Janeiro, RJ, Brasil*

For the DØ and CDF Collaborations

Hard diffraction in events with dijets and rapidity gaps has been studied by DØ and CDF for three processes: hard color singlet exchange, hard single diffraction, and hard double pomeron exchange, using Tevatron  $\bar{p}p$  data at  $\sqrt{s} = 630$  GeV and 1.8 TeV. Measurements of rates,  $\eta$ ,  $E_T$  and  $\sqrt{s}$  dependencies are presented and comparisons made with predictions of several models.

## I. INTRODUCTION

Events with a region of rapidity space devoid of particles (rapidity gaps) were first observed in cosmic ray data [1]. The idea of diffractive dissociation of projectile and target to produce such events soon followed [2]. Later the interpretation of total, elastic and diffractive cross sections in terms of the exchange of an object with the quantum numbers of the vacuum, called the pomeron, proved very useful [3]. F. Low and S. Nussinov suggested that the pomeron corresponds to the interchange of two gluons [4]. In a latter development Ingelman and Schlein (IS) proposed that high  $p_T$  jets could be diffractively produced via pomeron exchange and that this might probe the partonic structure of the pomeron [5]. Events containing rapidity gaps and jets were first observed by UA8 [6], giving rise to the field of hard diffraction. This area of interest has expanded considerably in the last decade, with the availability of high energy colliding beams. Jet production with rapidity gaps have been observed at the Tevatron [7,8] and at HERA [9]. CDF and DØ have studied dijet + rapidity gap events using data from the 1992-1996 Tevatron  $\bar{p}p$  collider run (Run I) at center-of-mass energy ( $\sqrt{s}$ ) = 1.8 TeV, with a short run at 630 GeV during that period. Because of the large center of mass energy and large integrated luminosity, the new CDF and DØ results can give further insight into diffractive processes.

The DØ detector is described elsewhere [10]. Jets are found in the uranium-liquid argon calorimeters using a cone algorithm with radius  $R = 0.7$  in the  $\eta - \phi$  plane [11]. Particle multiplicity is determined in the central region ( $|\eta| < 1.0$ ) using the number of towers ( $0.1 \times 0.1$  in  $\Delta\eta \times \Delta\phi$ ) with transverse energy ( $E_T$ ) above 200 MeV in the central electromagnetic calorimeter and the number of tracks in the central drift chamber. In the forward region this multiplicity is measured by the number of towers with ( $E_T$ ) above 125 MeV in the electromagnetic end cap calorimeter ( $2.1 < |\eta| < 4.1$ ) and 500 MeV in the hadronic end cap calorimeter ( $3.2 < |\eta| < 5.2$ ). Because the last layer of the hadronic calorimeter (at the limit of the forward acceptance) is composed of stainless steel and produces less noise than the uranium sections, the threshold for particle detection was reduced to 50 MeV in this layer. In addition, in the forward region we also use an array of scintillator hodoscopes, called LØ detector, to tag the presence of charged particles in the region  $2.3 < |\eta| < 4.3$ .

The CDF detector, described in ref. [12], consists of a large central detector with tracking in a solenoidal field and calorimetry over  $|\eta| < 4.2$ . To measure particle multiplicities, CDF uses the central tracker ( $|\eta| < 1.1$ ,  $p_T^{track} > 300$  MeV), the central calorimeter ( $|\eta| < 1.1$ ,  $E_T^{tower} > 300$  MeV corrected), and forward calorimeters ( $2.2 < |\eta| < 4.2$ ). For the last two months of the collider run, CDF installed three Roman Pot detectors to trigger on quasi-elastically scattered antiprotons. Nearly all the pot triggers have  $0.05 < \xi < 0.1$ , where  $\xi = 1 - x_F$  is the fraction of momentum lost by the antiproton and carried by the pomeron.

## II. HARD COLOR SINGLET EXCHANGE

Two jets separated by a rapidity gap has been proposed as the signature of color singlet exchange (CSE) carrying a high  $Q^2$  [13,14]. Rapidity gaps between jets have been observed both at the Tevatron [7] and at the DESY  $ep$  Collider (HERA) [9]. The measured rates of  $\approx 1\%$  at the Tevatron and  $\approx 10\%$  at HERA are too large to be accounted for by electroweak boson exchange and indicate a strong interaction process.

DØ and CDF have made recent studies of dijet data with central rapidity gaps. Both experiments measure the color singlet fraction ( $f_S$ ) at  $\sqrt{s}$  of 630 GeV and 1.8 TeV. The observed color singlet fraction includes the probability that the rapidity gap is not contaminated by particles from spectator interactions. This survival probability ( $S \sim 10\%$  at 1.8 TeV) is assumed to be independent of Bjorken  $x$  and the flavor of the initial partons in the hard scattering [17,18] but depends on  $\sqrt{s}$  ( $S_{630}/S_{1800} = 2.2 \pm 0.2$ ) [19].

CDF measures the fraction of colorless exchange to all opposite side dijets from the tracking distribution. Results are listed in Table II. The ratio of the CDF fractions from the measurements at the two center of mass energies is  $R(\frac{630}{1800}) = 2.4 \pm 0.9$ . No  $E_T$  dependence of the signal is observed.

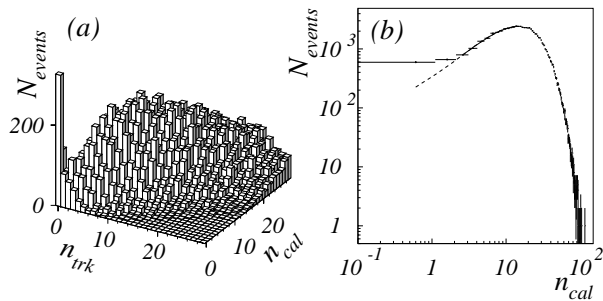


FIG. 1. The multiplicity between the dijets for the DØ high- $E_T$  1800 GeV sample: (a) two-dimensional multiplicity,  $n_{\text{cal}}$  vs.  $n_{\text{trk}}$ ; (b)  $n_{\text{cal}}$  only with NBD fit, plotted on a log-log scale to emphasize low multiplicity bins.

experiment	$\sqrt{s}$ (GeV)	jet $E_T$	$\eta^{\text{jet}}$	nb. of triggered events
CDF	630	> 8 GeV	$1.8 <  \eta  < 3.5$	1k + 1k(same-side)
DØ	630	>12 GeV	$ \eta  > 1.9$	7k
CDF	1800	>20 GeV	$1.8 <  \eta  < 3.5$	10k + 30k(same-side)
DØ	1800	>12 GeV	$ \eta  > 1.9$	48k
DØ	1800	>25 GeV	$ \eta  > 1.9$	21k
DØ	1800	>30 GeV	$ \eta  > 1.9$	72k

TABLE I. Kinematic cuts for color singlet exchange.

$f_S(\%)$	$E_T$ (GeV)	$\sqrt{s}$ (GeV)	experiment
$2.7 \pm 0.7$ (stat.) $\pm 0.6$ (syst.)	> 8	630	CDF
$1.85 \pm 0.09$ (stat.) $\pm 0.37$ (syst.)	> 12	630	DØ
$0.54 \pm 0.06$ (stat.) $\pm 0.16$ (syst.)	> 12	1800	DØ
$0.94 \pm 0.04$ (stat.) $\pm 0.12$ (syst.)	> 30	1800	DØ
$1.13 \pm 0.12$ (stat.) $\pm 0.11$ (syst.)	>20	1800	CDF

TABLE II. Color singlet Fractions .

DØ has recently published results for dijet + central gap events [20]. (See Table I for kinematic cuts.) Single interaction events are required. The particle multiplicity in the central rapidity region is approximated by the multiplicity,  $n_{cal}$ , of transverse energy above 200 MeV in the electromagnetic calorimeter, and by the track multiplicity in the central tracking chamber,  $n_{trk}$ . Figure 1 (a) shows the DØ multiplicity distribution for  $n_{cal}$  versus  $n_{trk}$ .

To calculate the fraction due to color singlet exchange, the leading edge of each  $n_{cal}$  distribution is fitted using a single negative binomial distribution (NBD). The fraction of rapidity gap events ( $f_S$ ) is calculated from the excess of events over the fit in the first two bins ( $n_{cal} = 0$  or 1) divided by the total number of entries. Figure 1 (b) shows the  $n_{cal}$  distribution and the NBD fit for the high  $E_T$  sample. See Table II for values of  $f_S$ . The DØ value of the ratio of the rapidity gap fractions at 630 and 1800 GeV is  $R(\frac{630}{1800}) = 3.4 \pm 1.2$ .

Measuring the color-singlet fraction as a function of  $E_T$ ,  $\eta$  and  $\sqrt{s}$  probes the nature of the color-singlet exchange and its coupling to quarks and gluons. If the color-singlet dynamics are similar to single gluon exchange except for different coupling factors to quarks and gluons, the color-singlet fraction would depend only on parton distribution functions via  $x_F$ . Thus for a color-singlet that couples more strongly to gluons than quarks, the color-singlet fraction would fall as a function of increasing  $x$ , since the gluon distribution becomes suppressed relative to the quark distribution as  $x$  increases. This implies a decreasing color singlet fraction with increasing jet  $E_T$  and  $\Delta\eta$  or decreasing  $\sqrt{s}$ .

To measure the color-singlet fraction as a function of  $E_T$  and  $\eta$ , DØ uses the two-dimensional multiplicity, ( $n_{cal}$  vs.  $n_{trk}$ ) which gives improved signal-to-background ratios compared to the NBD method. This is useful for smaller statistics samples and avoids large uncertainties in the color-exchange background subtraction. The “2D” color-singlet fraction  $f_{2D}$  is defined as the fraction of events with  $n_{cal} + n_{trk} < 2$ . The results are shown in Figure 2. The systematic errors include effects from background estimation. The measured color-singlet fraction shows a slight rise as a function of dijet  $E_T$  and  $\Delta\eta$ .

To compare the experimental color singlet fractions to models, DØ uses HERWIG 5.9 [21], which includes a two-gluon exchange with BFKL dynamics [15], and uses CTEQ2M parton distribution functions. In addition, DØ uses the  $t$ -channel photon exchange process in HERWIG to investigate models in which the color singlet couples only to quarks with a massless photon-like singlet.

In the soft-color rearrangement model [16], initial state quarks have fewer color combinations and thus, a higher probability of being rearranged into a colorless state, than initial state gluons, i.e.  $C_{gg} < C_{qg} < C_{qq}$ , where the “ $C_{abs}$ ” are the effective color factors representing the couplings to different initial state partons. A reasonable choice of color factors is  $C_{qq} = \frac{1}{9}$ ,  $C_{qg} = \frac{1}{24}$  and  $C_{gg} = (\frac{1}{64})$ . Predictions of these models are simultaneously fit to the experimental  $E_T$  and  $\Delta\eta$  dependence of  $f_S$  at  $\sqrt{s} = 1.8$  TeV, letting the normalization float. The results are shown in Figure 2. The data favour color-singlet models that couple more strongly to quarks than gluons, but a single-gluon model (no dependence) can not be excluded.

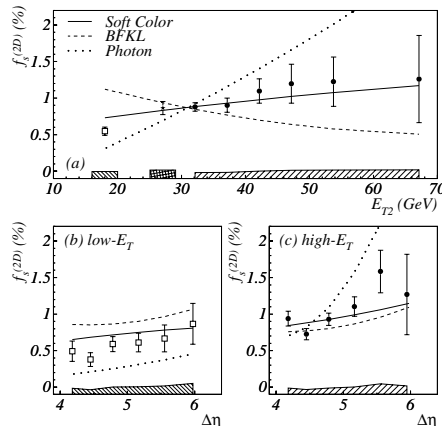


FIG. 2. Monte Carlo fits to the measured color-singlet fraction  $f_{2D}$ . The normalization is allowed to float.

### III. HARD SINGLE DIFFRACTION

In the IS picture of hard single diffraction, a pomeron (color singlet object) is emitted from the incident  $p$  ( $\bar{p}$ ) and undergoes a hard scattering with the  $\bar{p}$  ( $p$ ), leaving a rapidity gap in the direction of the parent particle. The signature is two jets produced on the same side and a forward rapidity gap along the direction of one of initial beam particles.

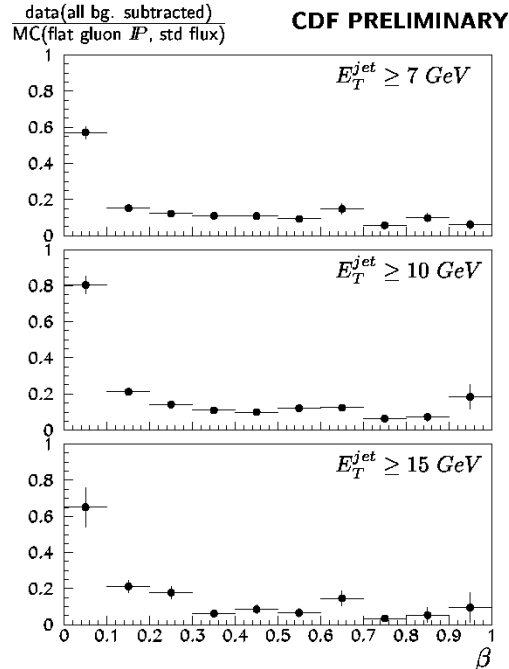


FIG. 3. Ratio of Data to Monte Carlo simulation as a function of  $\beta$  using a flat gluon distribution and standard pomeron flux

Data was taken by the CDF detector at the end of Run I using a trigger which requires tagging the recoil  $\bar{p}$  with “Roman Pot” detectors. The typical acceptance for these detectors is  $0.05 < \xi < 0.1$  and  $0 < |t| < 2 \text{ GeV}^2$ , where  $\xi$  is the fractional momentum lost by the antiproton and  $t$  its four momentum squared. After applying several cuts to select events with a good reconstructed track in the Roman Pots, CDF extracted the momentum fraction of the interacting parton in the pomeron,  $\beta$ , for dijet events with  $E_T > 7 \text{ GeV}$ , using the following expression:

$$\beta = \frac{E_T^{jet1} \exp(-\eta^{jet1}) + E_T^{jet2} \exp(-\eta^{jet2})}{2\xi P_{beam}} \quad (1)$$

The  $\beta$  distribution for the pomeron was obtained by subtracting several background contributions in the data, of which the most important are 1) non-diffractive dijet events accidentally overlapped with a Roman Pot hit, 2) meson exchange background and 3) double diffraction background. After subtracting these contributions from the data, then unfolding the detector acceptance by using simulations with a flat gluon distribution, the data was divided by Monte Carlo simulations based on POMPYT [22] using a flat gluon distribution and the standard Donnachie and Landshoff flux parametrization [23]. The comparison, shown in Figure 3, shows agreement in shape for  $\beta > 0.2$ , but there is a discrepancy in the normalization by about a factor of 6, as well as an enhancement for the low  $\beta$  region.

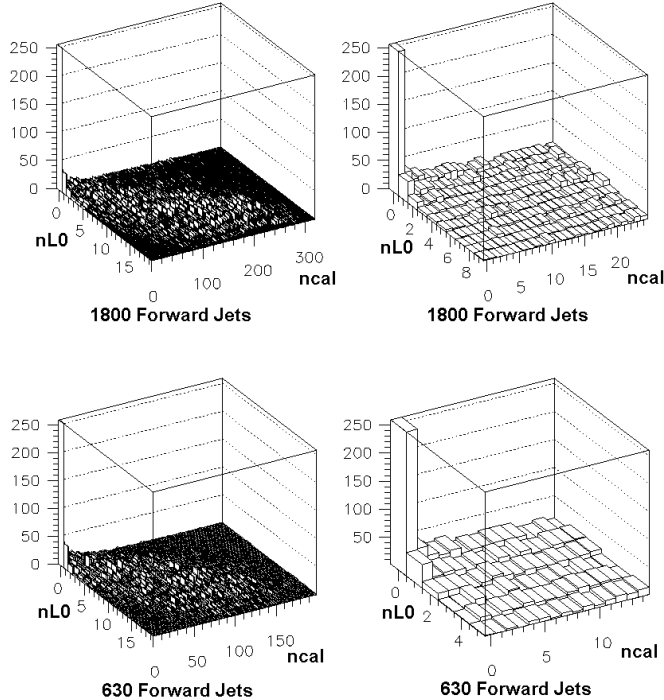


FIG. 4. Number of hits level 0 ( $n_{L0}$ ) and calorimeter towers ( $n_{CAL}$ ) above threshold opposite to jets in the forward trigger sample at center of mass energies 1800 and 630 GeV.

The  $D\bar{O}$  data were obtained using an inclusive jet trigger or a forward two jet trigger. Events are selected with two jets with  $E_T > 12$  GeV and  $|\eta| > 1.6$ . The number of end cap calorimeter towers ( $n_{cal}$ ) above threshold is measured opposite to the leading two jets. The  $n_{cal}$  distribution for the forward trigger sample at center of mass energies of 1800 and 630 GeV is shown in Figure 4. A clear peak is seen in the  $n_{L0} = n_{cal} = 0$  (zero multiplicity) bin as expected for a diffractive signal. A two-dimensional fit on the  $n_{L0}$  vs.  $n_{cal}$  distribution, where data and background are fit simultaneously, allows the direct extraction of the fraction of events containing a rapidity gap at both energies. This gap fraction, including statistical and systematic uncertainties, is determined to be  $0.64 \pm 0.05(stat. + syst.)\%$  for the 1800 GeV data and  $1.23 + 0.10 - 0.09(stat. + syst.)\%$  for the 630 GeV data. Work is in progress for the extraction of the pomeron parton distributions.

#### IV. HARD DOUBLE POMERON EXCHANGE

Central dijet events containing two rapidity gaps or a rapidity gap on the opposite side of a quasi-elastically scattered anti-proton have been studied by  $D\bar{O}$  and CDF respectively. This event topology is consistent with double pomeron exchange (DPE). The data can be used to give more information about the hypothesized pomeron.

CDF took data at 1800 GeV center of mass energy using the Roman Pot trigger to tag antiprotons. A sample of 27,000 events with a tagged  $\bar{p}$  and at least two jets with  $E_T > 7$  GeV is obtained. Low multiplicity events are selected by requiring  $N_{BBC}(west) \leq 6$  in the 16 element Beam-beam counters (BBC) on the same side as the pots. This gives 22,304 PJJ (pot-jet-jet) events. A sample of minimum bias events, with the same dijet selection, is used for comparison. Figure 5 (a) shows the calorimeter tower multiplicity in the east side (opposite to the pot track),  $N_{FCAL}$ , versus the number of hits in the BBC.

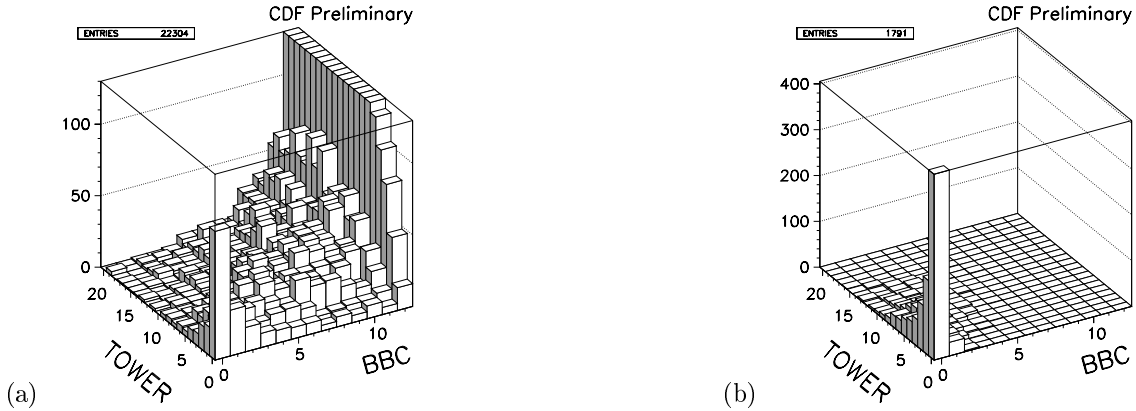


FIG. 5. (a) East side BBC vs Cal. tower multiplicity distribution for PJJ events, and 7 GeV dijets. (b) East side BBC vs Cal. tower multiplicity distribution for Monte Carlo Double Pomeron (with a flat  $\beta$  distribution.)

In order to understand the shape of this distribution, Monte Carlo events were generated using a version of POMPYP modified to include double pomeron exchange, where the incoming proton and antiproton emit pomerons with a standard flux (Donnachie and Landshoff form [23] with parameters as measured by CDF [24]). The pomeron-pomeron interaction is treated like a hadron hadron collision which produces jets. A flat  $\beta$  distribution of partons inside the pomeron was assumed. Diffractive deep inelastic scattering data from HERA suggest such a hard structure with a rather flat  $\beta$ -distribution [25]. The simulated events are shown in Figure 5 (b). The strong signal in the (0,0) bin only contains 24 % of the DPE events with  $\xi < 0.1$  for 7 GeV dijets.

By extrapolating linearly into the  $N_{BBC} = N_{FCAL} = 0$  bin along the diagonal axis, CDF obtained the ratio of dijet gap to dijet no-gap events to be:

$$R\left(\frac{PJJG}{PJJ}\right) = [0.36 \pm 0.05(stat.) \pm (0.03(syst.))]\%$$

where G means gap (no detected particles for  $2.4 < \eta < 5.9$ ), JJ means two jets with  $E_T > 7$  GeV and P means a pot track with  $0.05 < \xi < 0.1$ . When the discrepancy factor,  $D=18\%$ , found in previous analyses of diffraction in  $\bar{p}p$  and  $ep$  collisions [8], is applied (squared), the ratio from simulation is in good agreement with the data.

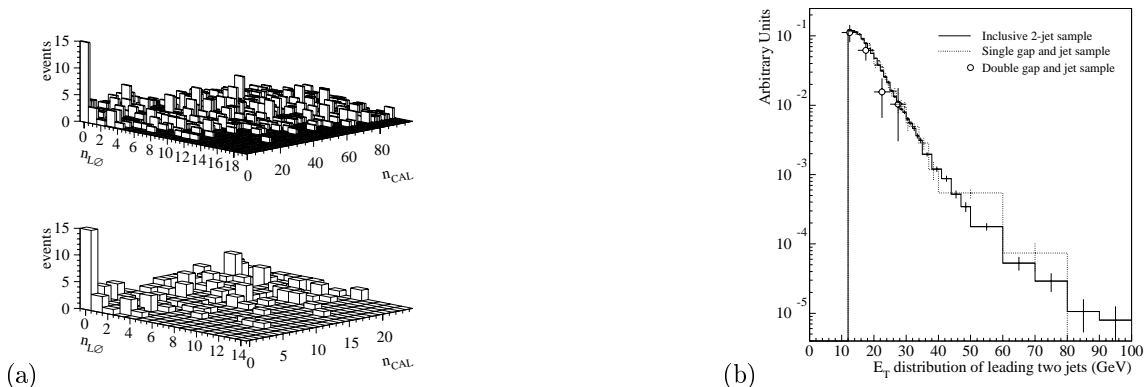


FIG. 6. (a) Multiplicity distribution of calorimeter towers ( $n_{cal}$ ) opposite a tagged rapidity gap for the 630 GeV  $D\bar{O}$  data. The bottom plot shows an expanded view of the low multiplicity region. (b)  $E_T$  distributions of the leading two jets for three data samples at 630 GeV. An inclusive sample requiring  $|\eta_{jet}| < 1.0$  is shown in the solid histogram. The distribution with the added requirement of one forward rapidity gap is shown with dotted lines and the distribution for double gap events is shown in circles.

$D\bar{O}$  has taken inclusive jet data with a special trigger and searched for dijet events with two forward rapidity gaps along the direction of the proton and antiproton. Events were selected having two jets with  $E_T > 12$  GeV,  $|\eta_{jet}| < 1.0$



and a rapidity gap in the region  $2.5 < |\eta| < 5.2$ . The multiplicity distribution of calorimeter towers and Level $\emptyset$  hits ( $n_{L\emptyset}$ ), on the opposite side to the rapidity gap, for data taken at 630 GeV center of mass energy is shown in Figure 6 (a). A clear peak at low multiplicity is observed above a fairly flat background in qualitative agreement with that expected for double pomeron exchange. Figure 6 (b) shows the  $E_T$  spectra for the two leading jets in an inclusive sample with two central  $E_T > 12$  GeV jets, a single forward gap sample and the double gap sample at 630 GeV. All three spectra are in good agreement where data are available, implying that the dynamics of leading jets produced in rapidity gap events appear similar to those of inclusive QCD production. Similar results are seen by D $\emptyset$  in data taken at 1800 GeV.

## V. CONCLUSIONS

Recent studies of hard diffraction at the Tevatron have given new information about rates of diffraction and dependencies on  $E_T$ ,  $\eta$  and  $\sqrt{s}$ .

The fraction of dijet events produced via hard color singlet exchange is about 1% at 1.8 TeV and is larger by a factor of 2 to 3 at  $\sqrt{s} = 630$  GeV. D $\emptyset$  has compared the  $E_T$  and  $\Delta\eta$  dependence of the fraction of hard color singlet events to several models. The data favor a soft-color rearrangement model preferring initial quark states over two-gluon color-singlet models.

CDF has preliminary results on the momentum distribution of partons in the pomeron using ‘‘Roman Pot’’ detectors to measure quasi-elastic scattered  $\bar{p}$  in hard single diffractive events. D $\emptyset$  has studied hard single diffraction in forward dijet events and new results on pomeron parton distributions will soon be available.

Both CDF and D $\emptyset$  have preliminary evidence for events with a hard double pomeron exchange topology. CDF has measured the fraction of pot dijet gap events to be 0.36% of the pot dijet events at  $\sqrt{s} = 1.8$  TeV. D $\emptyset$  has studied gap-dijet-gap events at  $\sqrt{s} = 630$  GeV and 1.8 TeV. The  $E_T$  distribution of the leading jets in double pomeron exchange type events is similar to other processes producing jets.

More detailed studies of the Tevatron data and further comparisons with models should give more insight into the nature of hard diffraction.

- [1] P. Ciok *et al.*, *Nuovo Cimento* **8**, 166 (1958); K. Niu, *Nuovo Cimento* **10**, 994 (1958); G. Cocconi, *Phys. Rev.* **111**, 1699 (1958).
- [2] M. Good and R. G. Walker *Phys. Rev.* **120**, 1857 (1960).
- [3] For a review see K. Goulianos, *Phys. Reports* **101**, 169 (1983).
- [4] F. Low, *Phys. Rev. D* **12**, 163 (1975); S. Nussinov, *Phys. Rev. D* **14**, 246 (1976).
- [5] G. Ingelman and P. Schlein *Phys. Lett. B* **152**, 256 (1985).
- [6] A. Brandt, *et al.*, *Phys. Lett. B* **297**, 417 (1992).
- [7] D $\emptyset$  Collaboration, S. Abachi *et al.*, *Phys. Rev. Lett.* **72**, 2332 (1994). CDF Collaboration, *Phys. Rev. Lett.* **74**, 855 (1995); D $\emptyset$  Collaboration, *Phys. Rev. Lett.* **76**, 734 (1996); CDF Collaboration, *Phys. Rev. Lett.* **80**, 1156 (1998).
- [8] CDF Collaboration, F. Abe *et al.*, *Phys. Rev. Lett.* **79**, 2636 (1997).
- [9] ZEUS Collaboration, M. Derrick *et al.*, *Phys. Lett. B* **369**, 55 (1996); ZEUS Collaboration, M. Derrick *et al.*, accepted for publication in *European Physics Journal* (1998).
- [10] D $\emptyset$  Collaboration, S. Abachi *et al.*, *Nucl. Instrum. Methods A* **338**, 185 (1994).
- [11] The pseudorapidity,  $\eta$  is defined as  $-\ln \tan(\theta/2)$ . The polar angle,  $\theta$ , is defined relative to the proton beam direction,  $\phi$  is the azimuthal angle, and  $E_T$  is the energy measured transverse to the beam.
- [12] CDF Collaboration, F. Abe *et al.*, *Nucl. Instrum. Methods A* **271**, 387 (1988).
- [13] Yu. L. Dokshitzer, V.A. Khoze and S.I. Troian, *Proceedings of the 6th International Conference on Physics in Collisions* (1986), ed. M. Derrick (World Scientific, 1987).
- [14] J.D. Bjorken, *Phys. Rev. D* **47**, 101 (1992).
- [15] A.H. Mueller and W.K. Tang, *Phys. Lett. B* **284**, 123 (1992).
- [16] O.J.P. Eboli, E.M. Gregores and F. Halzen, MAD/PH-96-965 (1997).

- [17] R.S. Fletcher and T. Stelzer, *Phys. Rev. D* **48**, 5162 (1993).
- [18] E. Gotsman, E.M. Levin and U. Maor, *Phys. Lett. B* **309**, 199 (1993).
- [19] E. Gotsman, E.M. Levin and U. Maor, TAUP 2485-98, hep-ph/9804404.
- [20] DØ Collaboration, B. Abbott *et al.*, *Phys. Lett. B* **440**, 189 (1998).
- [21] G. Marchesini, B.R. Webber, G. Abbiendi, I.G. Knowles, M.H. Seymour and L. Stanco, *Comp. Phys. Commun.* **67**, 465 (1992).
- [22] G. Ingelman, P. Bruni and A. Eden, POMPYT version 2.6
- [23] A. Donnachie and P. Landshoff, *Phys. Lett. B* **191**, 309 (1987); *Nucl. Phys. B* **303**, 634 (1988).
- [24] CDF Collaboration, F. Abe *et al.*, *Phys. Rev. D* **50**, 5518 (1994).
- [25] H1 Collaboration, T. Ahmed *et al.*, *Phys. Lett. B* **348**, 681 (1995); ZEUS Collaboration M. Derrick *et al.*, *Z. Phys. C* **68**, 569 (1995).